gate bias depletes the channel of holes, turning the device off. At low V_{DS}, the TFT shows typical transistor behavior as I_D increases linearly with V_{DS}. Current saturation, with only a small ohmic component, is observed at high V_{DS} as the accumulation of holes in the channel is pinched off near the drain electrode.

Device operation is adequately modeled by the standard field-effect transistor equations that apply to both organic and inorganic TFTs. From the plot of I_D and $I_D^{1/2}$ versus V_G (Fig. 3B) used to calculate current modulation (I_{ON}/I_{OFF}) and field-effect mobility, μ, in the saturation regime, the field-effect mobility for this device is 0.55 $cm^2/V \cdot s$ for a $\pm$50-V sweep of V_G at $V_{DS} \geq 60$ V. This mobility is typical for $(C_6H_5C_2H_4NH_3)_2SnI_4$ as it has been calculated for many devices on the same wafer, on different wafers, and from different preparations of the hybrid. These same device characteristics scale to smaller voltages as the gate oxide thickness is reduced. The highest mobility measured for this material, on a 1500 Å gate oxide at $V_{DS} = -30$ V, is 0.62 $cm^2/V \cdot s$, which is six times higher than that of any other spin-coated material (*4*) and comparable to a-Si and the best organic semiconductors deposited in high vacuum.

The field-effect mobility of these organic-inorganic TFTs depends on V_G (Fig. 3C) as reported for organic TFTs (*12*) and a-Si (*21*). Increasing V_G increases the number of accumulated charges available in the channel to fill localized traps in the material. At higher V_G, the trap states are filled, enabling additional charges to move with carrier mobilities defined by the delocalized bands of the hybrid semiconductor. Filling of trap states is likely responsible for the discontinuities shown in Fig. 3B, which suggests that higher mobilities may be achieved at lower V_G in TFTs with high dielectric gate insulators, which may be deposited on plastic substrates (*12*).

Materials that can be solution processed and exhibit a high I_{ON}/I_{OFF} are required for TFTs in low-cost large-area applications. The $(C_6H_5C_2H_4NH_3)_2SnI_4$ TFT (Fig. 3B) has an I_{ON}/I_{OFF} of $>10^4$. There is an increase in leakage as V_{DS} increases for large positive V_G, limiting the current modulation. These on-off ratios are achieved without patterning the semiconductor to the active region between source and drain electrodes. The hybrid is spun across a $\sim$1-cm^2 area of the wafer covering 16 devices. Patterning the semiconductor to the active device region reduces leakage through the insulator contributing to I_{OFF}, increasing I_{ON}/I_{OFF} to at least 10^6. Leakage, dominated by nonintentional dopants in unpatterned regions of the semiconductor away from the device, may be reduced by decreasing film thickness (*22*).

Organic-inorganic hybrid materials show the highest field-effect mobilities and I_{ON}/I_{OFF} ratios for spin-coated TFT channel materials. The cheap, low-temperature processing techniques suggest that organic-inorganic TFTs may be suitable for applications that require low cost, a large area, and the mechanical flexibility of plastic substrates. Semiconducting organic-inorganic hybrid materials may be designed with a wide range of organic and inorganic components for use in TFTs. Although $(C_6H_5C_2H_4NH_3)_2SnI_4$ has shown the best device characteristics, organic-inorganic perovskites with a tin(II) iodide framework and a variety of aliphatic (for example, alkyl-) and aromatic, ammonium, and diammonium cations have been incorporated in TFT devices and exhibit similar characteristics to those shown here. Increasing the dimensionality of the hybrid by increasing the number of repeated inorganic layers per organic layer may further increase film mobility. Improvements in materials processing and tailoring of the organic component are expected to increase mobilities in organic-inorganic TFTs with a SnI_2 framework up to at least 50 $cm^2/V \cdot s$. The flexibility in the chemistry of organic-inorganic hybrid materials may provide a path to preparation of both *n*-type and *p*-type transporting materials, which are necessary for complementary logic and normally "on" or "off" organic-inorganic TFTs.

References and Notes

1. A. R. Brown, A. Pomp, C. M. Hart, D. M. de Leeuw, *Science* **270**, 972 (1995).
2. C. D. Dimitrakopoulos, A. R. Brown, A. Pomp, *J. Appl. Phys.* **80**, 2501 (1996).
3. S. F. Nelson, Y. Y. Lin, D. J. Gundlach, T. N. Jackson, *Appl. Phys. Lett.* **72**, 1854 (1998).
4. P. T. Herwig, K. Müllen, *Adv. Mater.* **11**, 480 (1999).
5. G. Horowitz, D. Fichou, X. Peng, Z. Xu, F. Garnier, *Solid State Commun.* **72**, 381 (1989).
6. C. D. Dimitrakopoulos, B. Furman, T. Graham, S. Hegde, S. Purushothaman, *Synth. Met.* **92**, 47 (1998).
7. J. H. Burroughes, C. A. Jones, R. H. Friend, *Nature* **335**, 137 (1988).
8. A. Tsumura, H. Koezuka, T. Ando, *Appl. Phys. Lett.* **49**, 1210 (1986).
9. Z. Bao, A. Dodabalapur, A. J. Lovinger, *Appl. Phys. Lett.* **69**, 4108 (1996).
10. A. R. Brown, C. P. Jarrett, D. M. de Leeuw, M. Matters, *Synth. Met.* **88**, 37 (1997).
11. F. Garnier, R. Hajlaoui, A. Yassar, P. Srivastava, *Science* **265**, 1684 (1994).
12. C. D. Dimitrakopoulos, S. Purushothaman, J. Kymissis, A. Callegari, J. M. Shaw, *Science* **283**, 822 (1999).
13. For a review, see D. B. Mitzi, *Prog. Inorg. Chem.* **48**, 1 (1999).
14. D. B. Mitzi, C. A. Feild, Z. Schlesinger, R. B. Laibowitz, *J. Solid State Chem.* **114**, 159 (1995).
15. D. B. Mitzi, C. A. Feild, W. T. A. Harrison, A. M. Guloy, *Nature* **369**, 467 (1994).
16. C. Q. Xu *et al.*, *Solid State Commun.* **79**, 249 (1991).
17. K. Liang, D. B. Mitzi, M. T. Prikas, *Chem. Mater.* **10**, 304 (1998).
18. M. Era, T. Hattori, T. Taira, T. Tsutsui, *Chem. Mater.* **9**, 8 (1997).
19. D. B. Mitzi, M. T. Prikas, K. Chondroudis, *Chem. Mater.* **11**, 542 (1999).
20. G. C. Papavassiliou, I. B. Koutselas, A. Terzis, M. H. Whangbo, *Solid State Commun.* **91**, 695 (1994).
21. M. Shur, M. Hack, J. G. Shaw, *J. Appl. Phys.* **66**, 3371 (1989).
22. A. Dodabalapur, L. Torsi, H. E. Katz, *Science* **268**, 270 (1995).

23. We thank K. Chondroudis, J. Kymissis, and M. Prikas for technical assistance.

12 July 1999; accepted 23 September 1999

The Root of Angiosperm Phylogeny Inferred from Duplicate Phytochrome Genes

Sarah Mathews* and Michael J. Donoghue

An analysis of duplicate phytochrome genes (*PHYA* and *PHYC*) is used to root the angiosperms, thereby avoiding the inclusion of highly diverged outgroup sequences. The results unambiguously place the root near *Amborella* (one species, New Caledonia) and resolve water lilies (Nymphaeales, ~70 species, cosmopolitan), followed by *Austrobaileya* (one species, Australia), as early branches. These findings bear directly on the interpretation of morphological evolution and diversification within angiosperms.

The evolution of flowering plants fundamentally altered the biosphere. Deciphering the causes and consequences of their origin and radiation requires knowledge of phylogeny, especially the order in which branches diverged near the root of the tree (*1*). However, the root of angiosperms has remained unresolved, as different lines of evidence have suggested many disparate alternatives (*2*). This ambiguity stems in part from uncertainty surrounding the identity of their closest relatives (*3*–*5*), and from the great differences between angiosperms and all other living lines of seed plants. Such differences render homology assessments exceptionally difficult in morphological analyses, and may lead to "long branch attraction" in molecular analyses, which occurs when convergent nucleotide substitutions cause the spurious connection of highly diverged sequences (*6*). In analyses of angiosperms, distant outgroup sequences might connect (perhaps with confidence) to the most divergent angiosperm sequence or sequences. For this reason it has been suggested that the angiosperm root may never be resolved using nucleotide sequence

variation (*7*).

We used analysis of duplicate genes to root the angiosperm phylogeny without outgroups. This approach has been used to root the entire tree of life, for which outgroups are unknown (*8*). It seldom has been used elsewhere (*9*) but might be of general use, especially for rooting clades that are highly diverged from all known relatives. We reasoned that simultaneous analysis of members of a gene pair that duplicated along the line leading to extant angiosperms should yield an unrooted network of two identical (or very similar) gene subtrees connected by a single branch. If the subtrees are congruent, rooting the network along the connecting branch allows the network to fit into a rooted species tree without requiring additional hypotheses of gene duplication, sorting, or horizontal transfer events (*2*).

Phylogenetic analyses of phytochrome genes in green plants suggest that the phytochrome gene pair, *PHYA* and *PHYC*, diverged along the branch leading to angiosperms (*2, 10*). *PHYA* and *PHYC* are found in most angiosperms examined, whereas only one gene lineage related to this pair is known from other seed plants (*10, 11*). We obtained and analyzed *PHYA* and *PHYC* sequences from 26 angiosperms (*12*) representing most taxa previously suggested to be early-diverging lineages. Parsimony analysis yielded six shortest unrooted networks. The strict consensus of these networks best fits a rooted species tree in which *Amborella* is separate from all other angiosperms (Fig. 1). This rooting is strongly supported in both *PHYA* and *PHYC* subtrees (92% and 83% bootstrap support, respectively). *Nymphaea* + Cabombaceae (water lilies) and *Austrobaileya* diverge next in both subtrees; *Austrobaileya* branches first in the *PHYA* subtree with moderate support (66%), whereas *Nymphaea* + Cabombaceae, or a clade including all three taxa, branches first in the *PHYC* subtree.

Among the most parsimonious networks, the one shown in Fig. 1 maximizes identical components (A through Q) in the *PHYA* and *PHYC* subtrees. The remaining angiosperms diverge into a clade composed of magnoliids (H), within which winteroids (J) are sister to Piperales (K), and another clade (D) containing eudicots (G) and monocots + Chloranthus (E). Magnoliales (P) and Laurales (M) either form a clade (*PHYA* subtree) or are paraphyletic with respect to winteroids + Piperales (*PHYC* subtree). Bootstrap support for winteroids (J) and monocots (F) is relatively strong in the *PHYA* subtree (96% and 80%, respectively) but moderate in the *PHYC* subtree (66% and 78%), whereas support for Laurales (M) is strong in the *PHYC* subtree (100%) but weak in the *PHYA* subtree (57%). Conflicts between subtrees apparently are not significant (*13*).

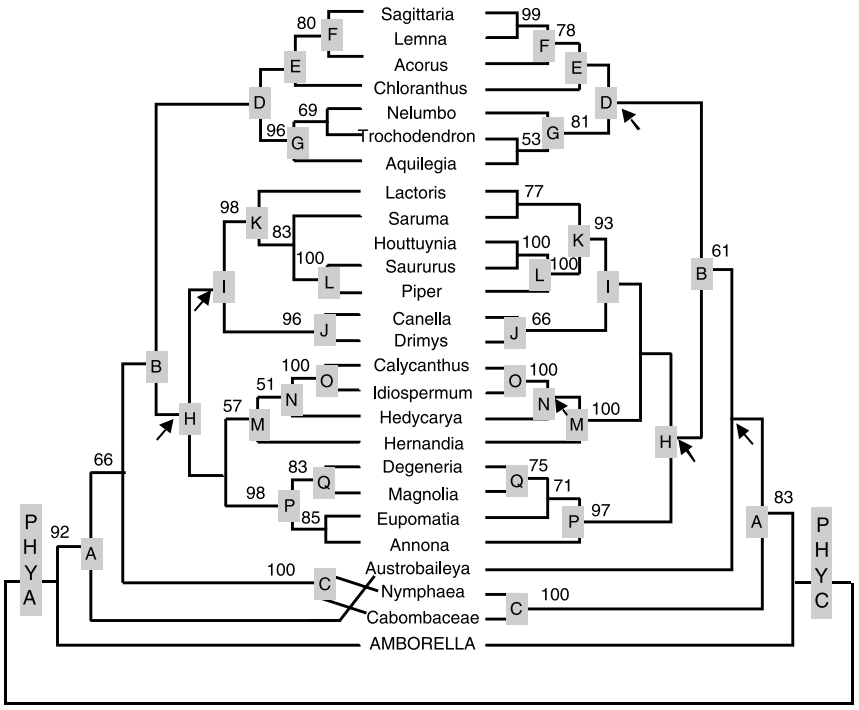

Fig. 1. One of the six most parsimonious networks of *PHYA* and *PHYC* from 26 angiosperms (1104 nucleotide sites, of which 634 are parsimony-informative). Heuristic parsimony analysis [100 random taxon addition replicates with tree bisection and reconnection swapping in PAUP* 4.0 (*33*)] yielded trees of 6423 steps [retention index (RI) = 0.50; consistency index (CI) = 0.24, excluding autapomorphies]. Identical components in the *PHYA* and *PHYC* subtrees are labeled A through Q. Bootstrap percentages (from 500 replicates with the same search parameters, but using 10 random addition replicates) are above branches. Arrows indicate branches that collapse in the strict consensus.

The duplicate gene analysis clearly resolves the angiosperm root along the branch to *Amborella*, and agreements between gene subtrees are many and strong. We therefore combined *PHYA* and *PHYC* data from each species for analysis, and rooted the resulting network by *Amborella*. Two most parsimonious trees resulted, which are identical except for the relative position of *Hernandia* and *Hedycarya* (Fig. 2). All clades in the consensus tree correspond to components resolved in one or both gene subtrees, and most are better supported. The two branches above *Amborella* are resolved with reasonably strong support; *Nymphaea* + Cabombaceae branch first, followed by *Austrobaileya* (bootstrap values of 80% and 86% for the remaining angiosperms, respectively).

Together, our phytochrome analyses provide insights into angiosperm phylogeny that were not evident in earlier studies. Other analyses have suggested at least nine different angiosperm rootings (*2, 14*), many with substantially different implications for angiosperm evolution. Only an analysis of 18*S* rDNA sequences (*15*) suggested a rooting near *Amborella*, but the result was equivocal. Results similar to ours are now being reported from analyses of large data sets that combine chloroplast, mitochondrial, and ribosomal sequences (*16–18*), or that combine many chloroplast sequences (*19*). This concordance implies that the question of the angiosperm root has been convincingly answered.

The conclusion that *Amborella*, water lilies, and *Austrobaileya* [which occurs in a clade with Illiciaceae and Schisandraceae (*14–18*) and *Trimenia* (*17, 20*)] form a grade at the base of the angiosperms has major implications for early evolution in flowering plants. Factors that may have contributed to their diversification include carpel closure (*21*), self-incompatibility (*22*), and the evolution of vessels (*23*). Our results imply that the carpels of the first angiosperms were sealed by secretions, and that postgenital fusion of epidermal layers evolved later (*24*). In our trees, *Chloranthus* and *Nelumbo* could represent reversions to closure by secretion; however, the placement of *Chloranthus* is only weakly supported. The conclusion that the first angiosperms were self-compatible plants (*25*) should be reexamined. Self-incompatibility has been noted in *Austrobaileya* and *Illicium*, implying either that it originated in the clade including these plants (probably early in angiosperm evolution) or

Department of Organismic and Evolutionary Biology, Harvard University Herbaria, 22 Divinity Avenue, Cambridge, MA 02138, USA.

*To whom correspondence should be addressed. E-mail: smathews@oeb.harvard.edu

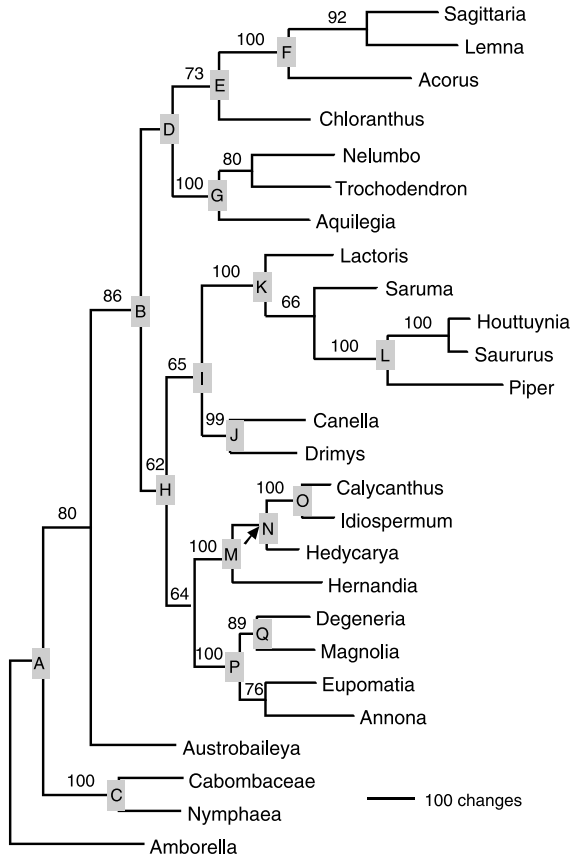

Fig. 2. Strict consensus of the two most parsimonious trees from analysis of concatenated *PHYA* and *PHYC* sequences (2208 nucleotide sites, of which 1042 are parsimony-informative), rooted at *Amborella* based on the duplicate gene analysis (Fig. 1). Heuristic parsimony analysis [100 random taxon addition replicates with TBR swapping in PAUP* 4.0 (*33*)] yielded trees of 6175 steps (RI = 0.36; CI = 0.38, excluding autapomorphies). Bootstrap percentages (from 500 replicates with the same search parameters, but using 20 random addition replicates) are above branches. Components identical with those found in both *PHYA* and *PHYC* subtrees are labeled A through Q. The arrow indicates the branch that collapses in the strict consensus.

that it was retained from the first angiosperms. Self-incompatibility may occur within water lilies, but the data are ambiguous (*25*). The condition in *Amborella*, with mostly unisexual flowers, is unknown, but possibly could be determined if functional stamens were found in otherwise carpellate flowers (*26, 27*). Our results suggest that xylem vessels evolved after the origin of the branch containing *Amborella*, which is vesselless. Vessels with small pores in the pit membranes are reported from most, but not all, water lilies (*28*), implying either that vessels originated (*28*) or were lost several times within water lilies. If the first water lilies had such vessels, they may have been transitional to typical vessels that lack pit membranes at maturity, perhaps through intermediates that retain remnants of pit membrane, as seen in Illiciaceae and Chloranthaceae (*29*). The absence of vessels in Winteraceae and the Trochodendronales may represent losses (*30*).

Our finding that the earliest branches within angiosperms are not species-rich could imply massive undetected extinction within these lineages. More likely it supports the conclusion that a shift in diversification rate did not coincide directly with the origin of flowering plants, but occurred later (*31*). Our results suggest that the first angiosperms probably were woody plants, in which case one or more shifts to the herbaceous habit may have fueled the major radiation of angiosperms.

References and Notes

1. J. A. Doyle and M. J. Donoghue, *Paleobiology* **19**, 141 (1993).
2. M. J. Donoghue and S. Mathews, *Mol. Phylogenet. Evol.* **9**, 489 (1998).
3. Analyses of morphological characters consistently suggest that Gnetales are the closest living relatives of angiosperms, but analyses of molecular data often unite Gnetales with conifers and support a clade of all extant seed plants except angiosperms [J. A. Doyle, *Int. J. Plant Sci.* **157**, S3 (1996); K.-U. Winter *et al., Proc. Natl. Acad. Sci. U.S.A.* **96**, 7342 (1999); A. Hansen, S. Hansmann, T. Samigullin, A. Antonov, W. Martin, *Mol. Biol. Evol.* **16**, 1006 (1999)].
4. S.-M. Chaw, C. L. Parkinson, Y. Cheng, T. M. Vincent, J. D. Palmer, *Proc. Natl. Acad. Sci. U.S.A.*, in press.
5. L. M. Bowe, G. Coat, C. W. dePamphilis, *Proc. Natl. Acad. Sci. U.S.A.*, in press.
6. J. Felsenstein, *Syst. Zool.* **27**, 401 (1978); J. Kim, *Syst. Biol.* **45**, 363 (1996).
7. M. W. Chase and A. V. Cox, *Aust. Syst. Bot.* **11**, 215 (1998).
8. N. Iwabe, K.-I. Kuma, M. Hasegawa, S. Osawa, T. Miyata, *Proc. Natl. Acad. Sci. U.S.A.* **86**, 9355 (1989); J. P. Gogarten *et al., Proc. Natl. Acad. Sci. U.S.A.* **86**, 6661 (1989); see also W. F. Doolittle and J. R. Brown, *Proc. Natl. Acad. Sci. U.S.A.* **91**, 6721 (1994).
9. T. Sang, M. J. Donoghue, D. Zhang, *Mol. Biol. Evol.* **14**, 994 (1997); M. J. Telford and P. W. H. Holland, *J. Mol. Evol.* **44**, 135 (1997); see also (*2*).
10. S. Mathews and R. A. Sharrock, *Plant Cell Environ.* **20**, 666 (1997).
11. Analyses of complete coding sequences from land plants place *PHY* from angiosperms in four independent gene lineages, each comprising homologs of *Arabidopsis PHYA*, *PHYB/D*, *PHYC*, or *PHYE* [all supported by bootstrap values of 100% (*10*)], and *PHY* from conifers in two gene lineages, one that diverges before divergence of *PHYB/D* from *PHYE*, and another that diverges before divergence of *PHYA* from *PHYC* [supported by bootstrap values of 100% and 74%, respectively (*2*)]. Phylogenies that include partial sequences from conifers, ginkgo, cycads, and Gnetales also resolve just two gene lineages in nonangiosperms, but the *PHYA*/*PHYC*-related lineage is equivocally resolved. Some analyses place it on the branch to *PHYA*, others on the branch to *PHYC*, but neither position is supported [H. A. W. Schneider-Poetsch, Ü. Kolukisaoglu, D. H. Clapham, J. Hughes, T. Lamparter, *Physiol. Plant.* **102**, 612 (1998); S. Mathews, unpublished data]. Thus, divergence of *PHYA* from *PHYC* before the origin of any nonangiosperm group is not supported. *PHYC* may have been lost from some eudicot lineages (*32*) [G. T. Howe *et al.*, *Mol. Biol. Evol.* **15**, 160 (1998)] and *PHYA* has diversified in others (*10, 32*). Diversification or loss of *PHYA* or *PHYC* (or both) has not been detected in early-diverging angiosperms except for *Ceratophyllum* (*10*), which is excluded from these analyses.
12. Locus-specific (*PHYA* upstream: 5′-CCYTAYGARGRNCCYATGACWGC-3′, 5′-GACTTTGARCCNGTBAAGCCTTAYG-3′; *PHYC* upstream: 5′-GAYTTRGARCCWGTDAAYC-3′; *PHYA* downstream: 5′-GDATDGCRTCCATYTCRTAGTC-3′, 5′-GTYTCMATBARDCKRACCATYTC-3′; *PHYC* downstream: 5′-GRATKGCATCCATYTCMAYRTC-3′) or degenerate oligonucleotides [upstream: 5′-TCWGGNAARCCNTTYTAYGC-3′, 5′-CCITTYTAYGSIATHYTICAYMG-3′; downstream: 5′-GTMACATCTTGRSCMACAAARCAYAC-3′, 5′-GCWGTRTGNGAYCTRAACCA-3′ (I, inosine; R, Y, M, K, S, W, H, B, D, and N correspond to the IUPAC-IUB ambiguity set); see also S. Mathews, M. Lavin, R. A. Sharrock, *Ann. Missouri Bot. Gard.* **82**, 296 (1995)] primed synthesis of 1- to 1.2-kb fragments of exon I using stepdown protocols [K. H. Hecker and K. H. Roux, *Biotechniques* **20**, 478 (1996)]. Fragments were cloned into pGEM-T Easy (Promega). No *PHYA* clones were obtained from *Lemna* or *Houttuynia*; a 330–base pair *PHYA* clone was obtained from *Hedycarya*. The data matrix of 1104 nucleotide sites comprised sequences of 24 *PHYA* and 26 *PHYC* clones. Cabombaceae is represented by *Brasenia* (*PHYA*) or *Cabomba* (*PHYC*). We obtained a 1.2-kb clone of just one of the *PHYA* copies in *Ceratophyllum* (*11*); its homology with other *PHYA* in our analyses could not be assessed without the second copy, so we excluded it from analyses. Available sequences from *Arabidopsis* and *Sorghum* are highly diverged from those analyzed here and were excluded from final analyses; their inclusion did not alter tree topologies but decreased bootstrap support for several branches, including eudicots and monocots. When they were included in analyses of fewer species, gene subtrees were rooted at *Sorghum* (*2*), a topology likely resulting from long branch attraction. GenBank accession numbers of sequences analyzed here are AF190060 to AF190109. Data matrices analyzed in this study are available from the first author and from TreeBASE (http://phylogeny.harvard.edu/treebase, SN295).
13. Results of Wilcoxon signed rank tests [see A. Larson, in *Molecular Ecology and Evolution: Approaches and Applications*, B. Schierwater, B. Street, G. P. Wagner, R. DeSalle, Eds. (Birkhäuser, Basel, Switzerland, 1994), pp. 371–390] indicate that *PHYA* and *PHYC* data sets are compatible with *PHYC* and *PHYA* subtrees, respectively ($P > 0.1$). Partition-homogeneity tests [J. S. Farris, M. Källersjö, A. G. Kluge, C. Bult, *Syst. Biol.* **44**, 570 (1995)] fail to reject the null hypothesis that *PHYA* and *PHYC* data sets are homogeneous ($P = 0.09$).
14. W. I. Nandi, M. W. Chase, P. K. Endress, *Ann. Missouri Bot. Gard.* **85**, 137 (1998); S. B. Hoot, S. Magallon, P. R. Crane, *Ann. Missouri Bot. Gard.* **86**, 1 (1999).
15. D. E. Soltis *et al.*, *Ann. Missouri Bot. Gard.* **84**, 1 (1997).
16. P. S. Soltis, D. E. Soltis, M. W. Chase, *Nature*, in press.
17. Y.-L. Qiu, J. Lee, F. Bernasconi-Quadroni, D. E. Soltis, P. S. Soltis, M. Zanis, E. A. Zimmer, Z. Chen, V. Savolainen, M. W. Chase, *Nature*, in press.
18. C. L. Parkinson, K. L. Adams, J. D. Palmer, in preparation.
19. S. W. Graham and R. G. Olmstead, unpublished data.
20. S. S. Renner, *Am. J. Bot.* **86**, 1301 (1999).
21. J. A. Doyle and M. J. Donoghue, *Bot. Rev.* **52**, 321 (1986).
22. H. L. K. Whitehouse, *Ann. Bot.* **14**, 199 (1950).

23. S. Carlquist, *Ecological Strategies of Xylem Evolution* (Univ. of California Press, Berkeley, CA, 1975).
24. A. Igersheim and P. K. Endress, *Bot. J. Linn. Soc.* **124**, 213 (1997); P. K. Endress and A. Igersheim, *Bot. J. Linn. Soc.* **125**, 93 (1997); A. Igersheim and P. K. Endress, *Bot. J. Linn. Soc.* **127**, 289 (1998).
25. S. J. Weller, M. J. Donoghue, D. Charlesworth, in *Experimental and Molecular Approaches to Plant Biosystematics*, P. C. Hoch and A. G. Stephenson, Eds. (Missouri Botanical Garden, St. Louis, MO, 1995), pp. 355–382.
26. P. K. Endress, unpublished data.
27. L. B. Thein, unpublished data.
28. E. L. Schneider and S. Carlquist, *Am. J. Bot.* **83**, 1236 (1996).
29. S. Carlquist, *Am. J. Bot.* **79**, 660 (1992).
30. D. A. Young, *Syst. Bot.* **6**, 313 (1981); M. J. Donoghue, *Evolution* **43**, 1137 (1989); T. S. Feild, M. A. Zwieniecki, M. J. Donoghue, N. M. Holbrook, *Proc. Natl. Acad. Sci. U.S.A.* **95**, 14256 (1998).
31. M. J. Sanderson and M. J. Donoghue, *Science* **264**, 1590 (1994).
32. M. Lavin, E. Eshbaugh, J.-M. Hu, S. Mathews, R. A. Sharrock, *Am. J. Bot.* **85**, 412 (1998).
33. D. L. Swofford, *PAUP* 4.0* (Sinauer Associates, Sunderland, MA, 1999).
34. We thank J. Doyle, P. Endress, L. Thein, P. Soltis, S. Graham, Y.-L. Qiu, J. Palmer, and C. dePamphilis for helpful discussions and for sharing unpublished data, and C. Soohoo and C. Davis for technical support. Financial support was provided by NSF grant DEB-9806937.

2 September 1999; accepted 1 October 1999

A Species of Small Antisense RNA in Posttranscriptional Gene Silencing in Plants

Andrew J. Hamilton and David C. Baulcombe*

Posttranscriptional gene silencing (PTGS) is a nucleotide sequence–specific defense mechanism that can target both cellular and viral mRNAs. Here, three types of transgene-induced PTGS and one example of virus-induced PTGS were analyzed in plants. In each case, antisense RNA complementary to the targeted mRNA was detected. These RNA molecules were of a uniform length, estimated at 25 nucleotides, and their accumulation required either transgene sense transcription or RNA virus replication. Thus, the 25-nucleotide antisense RNA is likely synthesized from an RNA template and may represent the specificity determinant of PTGS.

Posttranscriptional gene silencing occurs in plants and fungi transformed with foreign or endogenous DNA and results in the reduced accumulation of RNA molecules with sequence similarity to the introduced nucleic acid (*1*, *2*). Double-stranded RNA induces a similar effect in nematodes (*3*), insects (*4*), and protozoa (*5*). PTGS can be suppressed by several virus-encoded proteins (*6*) and is closely related to RNA-mediated virus resistance and cross-protection in plants (*7*, *8*). Therefore, PTGS may represent a natural antiviral defense mechanism and transgenes might be targeted because they, or their RNA, are perceived as viruses. PTGS could also represent a defense system against transposable elements and may function in plant development (*9*–*11*).

To account for the sequence specificity and posttranscriptional nature of PTGS, it has been proposed that antisense RNA forms a duplex with the target RNA, thereby promoting its degradation or interfering with its translation (*12*). If these hypothetical antisense RNA molecules are of a similar size to typical mRNAs, they would have been readily detected by routine RNA analyses. However, there have been no reports of such antisense RNA that is detected exclusively in plants or animals exhibiting PTGS. Nevertheless, PTGS-specific antisense RNA may exist, but may be too short for easy detection. We carried out analyses specifically to detect low molecular weight antisense RNA in four classes of PTGS in plants (*13*). The first class tested was transgene-induced PTGS of an endogenous gene ("cosuppression"). We used five tomato lines (T1.1, T1.2, T5.1, T5.2, and T5.3), each transformed with a tomato 1-aminocyclopropane-1-carboxylate oxidase (ACO) cDNA sequence placed downstream of the cauliflower mosaic virus 35*S* promoter (35*S*). Two lines (T5.2 and T5.3) exhibited PTGS of the endogenous ACO mRNA (Fig. 1A). Low molecular weight nucleic acids purified from the five lines were separated by denaturing polyacrylamide gel electrophoresis, blotted, and hybridized to an ACO sense (antisense-specific) RNA probe (Fig. 1B). A discrete, ACO antisense RNA (*14*) of 25 nucleotides (nt) was present in both PTGS lines but absent from the nonsilencing lines. Twenty-five–nucleotide ACO RNA of sense polarity and at the same abundance as the 25-nt ACO antisense RNA was also present only in the PTGS lines (Fig. 1C).

PTGS induced by transgenes can also occur when a transgene does not have homology to an endogenous gene (*1*). Therefore, we tested whether this type of PTGS was also associated with small antisense RNA. We analyzed three tobacco lines carrying 35*S*-β-glucuronidase (GUS) transgenes. Two of these lines, T4 (*15*) and 6b5 (*16*), exhibited PTGS of GUS. The third line (6b5×271) tested was produced by crossing 6b5 with line 271 (*17*), in which there is a transgene suppressor of the 35*S* promoter in 6b5. There was no PTGS of GUS in 6b5×271 because of the transcriptional suppression of the 35*S* GUS transgene (*18*). Hybridization with a GUS-specific probe revealed that low molecular weight GUS antisense RNA was present in T4 and 6b5 (Fig. 2, lanes 1 and 2) but absent from line 6b5×271 (Fig. 2, lane 3). The amount of antisense RNA correlated with the extent of PTGS: Line 6b5 has stronger PTGS of GUS than line T4 (*18*) and had more GUS antisense RNA (Fig. 2).

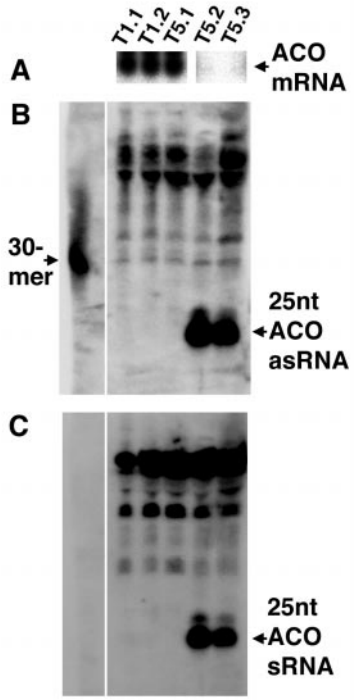

Fig. 1. Twenty-five–nucleotide ACO antisense and sense RNA in PTGS lines. (**A**) Endogenous ACO mRNA abundance in five tomato lines containing 35*S*-ACO transgenes. ACO mRNA was amplified by reverse transcriptase–polymerase chain reaction and detected by hybridization with labeled ACO cDNA. (**B** and **C**) Low molecular weight RNA from the same five lines and a 30-nt ACO antisense RNA were fractionated, blotted, and hybridized with either ACO sense RNA (**B**) or antisense RNA (**C**) transcribed from full-length ACO cDNA. The low hybridization temperature permitted some nonspecific hybridization to tRNA and small ribosomal RNA species, which constitute most of the RNA mass in these fractions. The oligonucleotide hybridized only to the antisense-specific probe (**B**). Twenty-five–nucleotide, PTGS-specific RNA is indicated.

Sainsbury Laboratory, John Innes Centre, Colney Lane, Norwich NR4 7UH, UK.

*To whom correspondence should be addressed. E-mail: david.baulcombe@bbsrc.ac.uk